Int. J. Rock Mech. Min. Sci. & Geomech. Abstr. Vol.30, No.7, pp. 1387–1393, 1993
Printed in Great Britain

0148-9062/93 $6.00 + 0.00
Pergamon Press Ltd

Geotechnical Applications of a Two-Dimensional Elastodynamic Displacement Discontinuity Method

E. SIEBRITS[1]
S.L. CROUCH[2]

A general two-dimensional elastodynamic displacement discontinuity method is used to model a variety of application problems. The plane strain problems are: the elastodynamic motions induced on a cavity by shear slip on a nearby crack; the dynamic response of a backfilled versus a non-backfilled tabular excavation or stope; and the interaction between two inclined stopes and a slipping fault. An antiplane strain problem is also presented, where slip occurs along a crack near the surface of a half plane. These problems indicate the wide potential of this method in investigating elastodynamic effects, especially for crack-like geometries.

INTRODUCTION

Elastostatic boundary element methods are routinely used in the mining industry to investigate the effects of different mining layouts on the displacements and stresses in the surrounding rock mass. Many important practical problems, however, involve transient phenomena, which cannot be taken into account in static analyses. Elastodynamic methods can be used, for example, to determine the effects within a rock mass of sudden changes in the mining layout, or to observe the interactions between seismic waves generated by slip along a fault, and mining excavations. Valuable information about the particle velocities, accelerations, displacements, and stresses can be obtained from an elastodynamic model.

The displacement discontinuity method is well established in elastostatics [1]. In elastodynamics, two- and three-dimensional boundary integral methods have been developed to solve crack-like problems [2, 3, 4, 5]. These methods all use numerical integrations at some stage of the derivation. The development of displacement discontinuity methods in three and two dimensions, using analytical integrations in both space and time have also been developed [6, 7].

A number of geotechnical applications of a two-dimensional elastodynamic displacement discontinuity method, called TWO4D [7], are presented in this paper, demonstrating the potential of this method. A brief summary of the mathematical background follows, as well as a validation of the numerical model with an analytical solution in order to demonstrate the accuracy of this method. Further validations are available [7].

1. Mining Technology Division, CSIR, P. O. Box 91230, Auckland Park, 2006, Republic of South Africa.
2. Department of Civil and Mineral Engineering, University of Minnesota, 500 Pillsbury Drive S.E., Minneapolis, MN 55455-0220, U.S.A.

MATHEMATICAL BACKGROUND

The elastodynamic displacement discontinuity method is a boundary element method designed for crack-like or tabular geometries in an infinite, homogeneous, isotropic, and linearly elastic domain. The method solves for the shear and normal discontinuities in displacement, due to a known history of shear and normal tractions, on a crack surface. Once the displacement discontinuity components have been determined, time histories of displacements, particle velocities, and stresses can be calculated at arbitrary field positions in the surrounding continuum.

The method can be summarized in the following boundary integral equations, which describe the displacements $u_k(\underline{x},t)$ and stresses $\sigma_{kl}(\underline{x},t)$ at position $\underline{x}$ and time t in terms of the displacement discontinuities $D_i(\underline{\xi},t)$ at position $\underline{\xi}$ convoluted with fundamental solutions $T_{ki}(\underline{x},t;\underline{\xi},0)$ and $S_{klij}(\underline{x},t;\underline{\xi},0)$, respectively

$$u_k(\underline{x},t) = \int_S T_{ki}(\underline{x},t;\underline{\xi},0) * D_i(\underline{\xi},t) dS(\underline{\xi}) \qquad (1)$$

$$\sigma_{kl}(\underline{x},t) = \int_S S_{klij}(\underline{x},t;\underline{\xi},0) * D_i(\underline{\xi},t) n_j dS(\underline{\xi}) \qquad (2)$$

The * symbol in the above equations is the time convolution operator [8], and denotes a time integration between the fundamental solution and the displacement discontinuity function. The fundamental solutions T_{ki} and S_{klij} describe the displacements and stresses, respectively, due to the spatial derivative of a unit impulse in space and time [8]. These fundamental solutions therefore describe a dynamic doublet state [8]. In three dimensions, all indices range from 1 to 3. In the two-dimensional case, indices range from 1 to 2 for the in-plane part, and the third index is the antiplane part. The two-dimensional fundamental solution is obtained from the three-dimensional one by spatial integration in

the antiplane direction [8].

In order to obtain the two-dimensional numerical method, the spatial integrals are discretized into linear elements with a piecewise linear variation of the displacement discontinuity functions over each element and internal collocation. The time integrals are discretized into time steps, with a linear variation in the displacement discontinuity functions within each time step. All space and time integrations are performed analytically, resulting in a set of algebraic equations in an implicit time-marching algorithm given by [9]

$$\underline{b}^m = \underline{C}^1 \underline{D}^m + \sum_{k=1}^{m-1} \underline{C}^{m-k+1} \underline{D}^k \qquad (3)$$

where

m = current time step number
$\underline{C}$ = influence coefficient matrix
$\underline{b}$ = vector of known boundary displacements and/or tractions
$\underline{D}$ = vector of displacement discontinuities.

The above equation can be structured so that, in general, a mixed displacement and/or traction boundary value problem can be solved for the unknown shear and normal displacement discontinuities $\underline{D}^m$ at the current time step m. The summation term contains a history of known influences from previous time steps.

SUDDENLY PRESSURIZED SEMI-INFINITE CRACK

An analytical solution [10] exists for the case of a stationary, suddenly pressurized semi-infinite crack, as depicted in Figure 1, under plane-strain conditions.

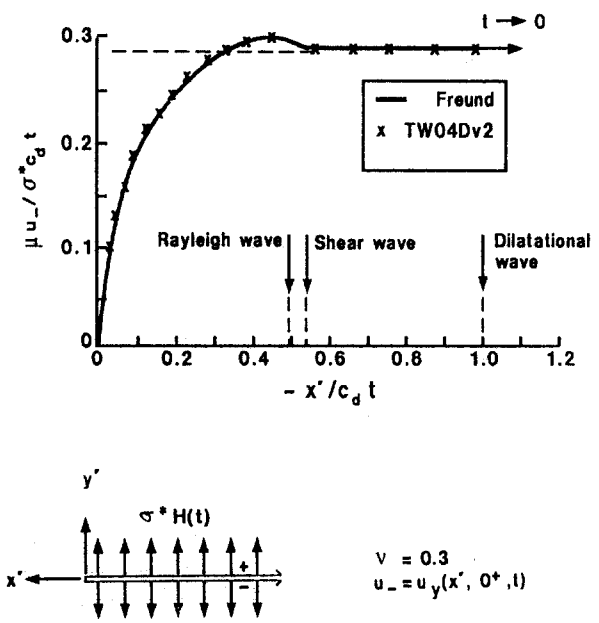

Figure 1. Normalized normal displacement of upper crack face versus normalized distance (after Freund [10]).

Figure 1 shows a normalized crack face displacement versus normalized "distance" plot of the analytical solution and the numerical solution obtained using TWO4D. The numerical solution matches the analytical solution until the first diffracted wave arrivals from the truncated row of displacement discontinuity elements (total length L), used to approximate the semi-infinite crack, at time $t = (L + x')/c_d$, where c_d is the compressional wave velocity.

Before the arrival of the compressional waves from the crack edge, all applicable positions along the crack faces are governed only by the applied crack pressure, indicated by the horizontal dashed line in Figure 1. Notice that the peak motions coincide with the arrival of the Rayleigh wave along the crack faces.

CAVITY RESPONSE DUE TO SHEARING CRACK

The interaction between the stress waves generated from a displacement discontinuity shear source and a large cavity is modeled here. A similar problem has also been modeled in three dimensions [11], using an elastodynamic fictitious stress method.

A cavity (or exterior) problem can be modeled with the displacement discontinuity method, but care should be taken to prevent rigid body motions of the interior [1]. This can be accomplished either by introducing extra displacement discontinuity elements inside the cavity and prescribing zero shear and normal displacements on one side of each of those elements, or by leaving a small section along the cavity boundary undiscretized so that the interior and exterior are connected together. The first approach requires the solution of a mixed boundary value problem (displacement and traction), and the latter approach allows stress waves to enter the cavity naturally via the connecting bridge. Both approaches give satisfactory results (the former approach is presented here). Care should be taken to use a sufficiently fine discretization to prevent excessive numerical leakage of the stress waves directly through the mesh into the cavity. The resolution required depends upon the temporal and spatial variation of the source loading - a load applied abruptly over a short distance generates high frequencies and hence a fine discretization is needed.

Figure 2 depicts the geometry and loading of a cavity that interacts with stress waves from a nearby slipping crack. Figures 3 and 4 are snapshots in time of the dynamic displacements and particle velocities, plotted in a vertical window, induced by the slipping crack. Notice that the left and bottom sides of the cavity experience significant motion, even though they are on the leeward side of the source. Different orientations of the shear source with respect to the cavity would result in quite different dynamic responses.

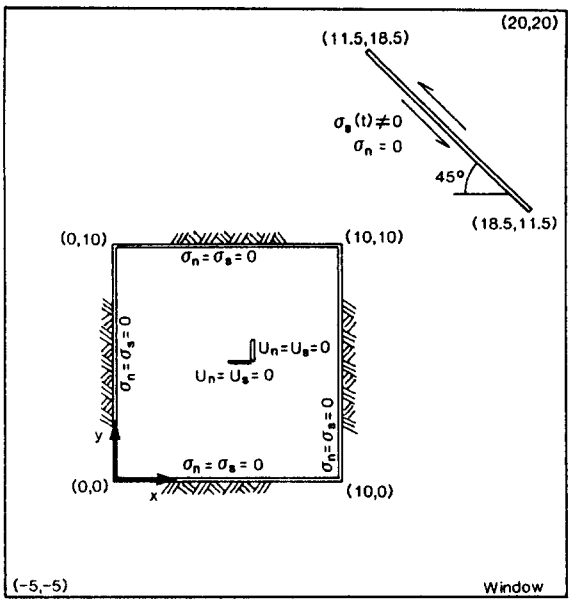

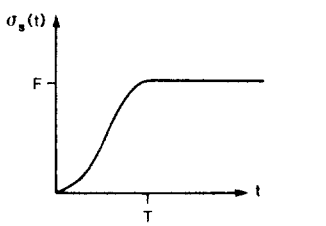

E = 70 GPa
υ = 0.2
ρ = 2700 kg/m^3
Q1 = 0.6
ΔX = 1 m

T = 2 ms
F = 100 MPa
If t<T, $\sigma_s(t) = F\left(\frac{t}{T}\right)^2 \left(3 - 2\frac{t}{T}\right)$

Figure 2. Geometry and loading of cavity problem.

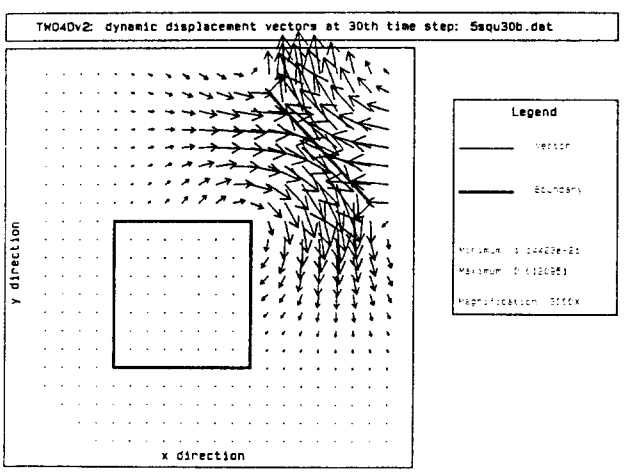

Figure 3a. Snapshot in time of induced dynamic displacement vectors.

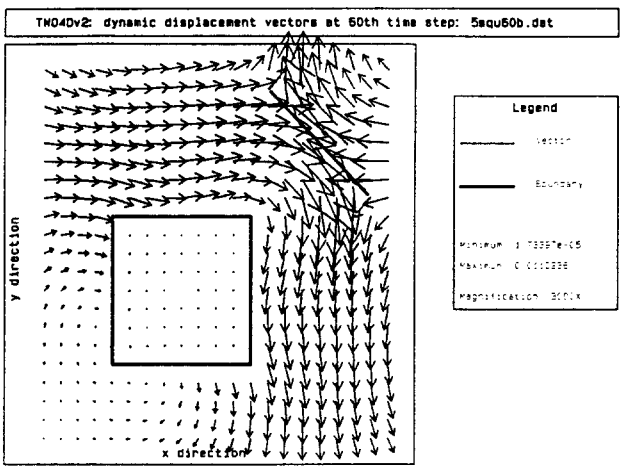

Figure 3b. Snapshot in time of induced dynamic displacement vectors.

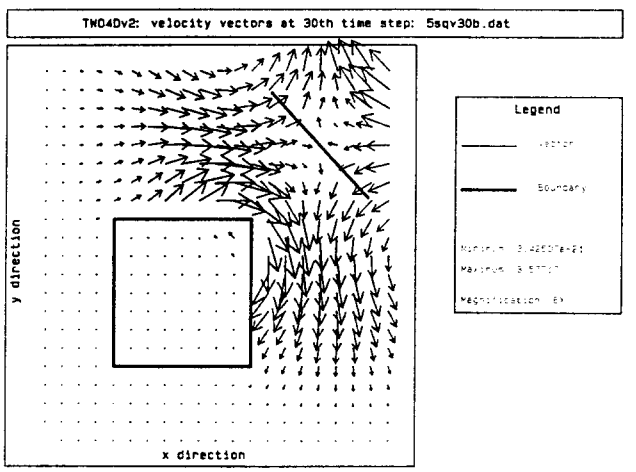

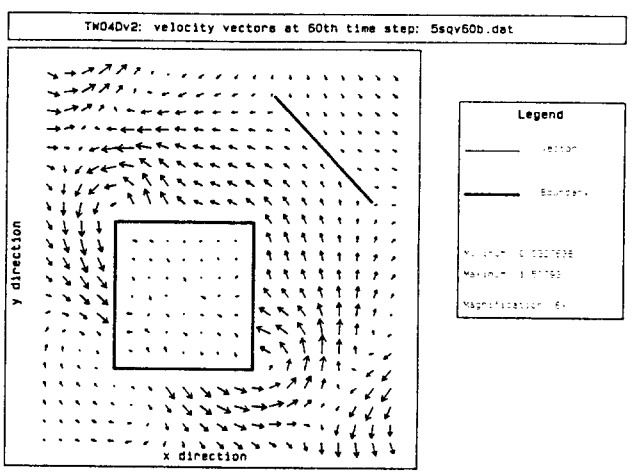

Figure 4. Snapshots in time of particle velocities.

STRESS WAVE INTERACTION WITH FILLED AND UNFILLED STOPE

Deep-level gold mines in the Witwatersrand of South Africa experience a high level of seismicity. The gold reef typically occurs in extensive tabular deposits. It is often possible to approximate the effect of these excavations in the surrounding rock mass by assuming plane strain. As mining proceeds, the stresses are changed in the surrounding rock mass. After a sufficient build-up of stress, a seismic event can occur by failure of the intact rock or along weaker faults or pre-existing mining induced fractures. In order to reduce rockburst and rockfall damage, the mined out sections of the stope are often filled with finely crushed waste rock, called backfill.

There is almost no experimental data available about the dynamic constitutive response of backfill. Hence, so-called "seam" elements [1] are used here in an attempt to model backfill. Each displacement discontinuity seam element contains shear and normal springs with a linear force-displacement response (Figure 5).

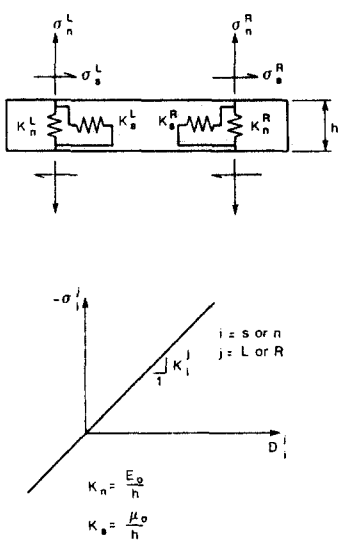

Figure 5. Seam element and loading response.

Figure 6 depicts a problem where a stope is modeled with and without backfill. The dynamic spring stiffnesses are assumed to be K_S = 200 MPa/m and K_n = 400 MPa/m. The elastic constants of E = 35 GPa, ν = 0.27, and ρ = 2,700 kg/m^3 are different to the usual values used for quartzitic rock. The soft Young's modulus is used in order to try to account for the highly fractured nature of the rock mass around a deep-level stope, in an elastic analysis [12].

Figure 7 shows velocity vector snapshots in time of the interaction of the elastic waves generated by the shear source with the filled stope. The dominant motions are generated after the arrival of the shear waves because the source is of a shearing nature. In Figure 7a the largest particle velocity vectors are those coinciding with the arrival of the Rayleigh wave along the stope.

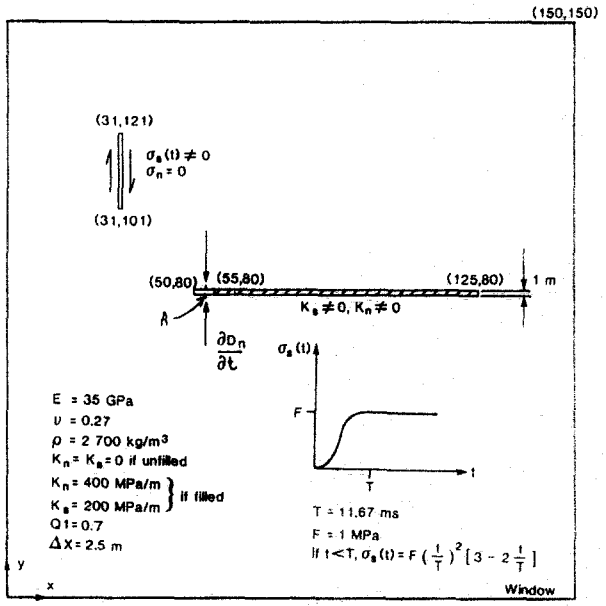

Figure 6. Geometry and loading of filled/unfilled stope.

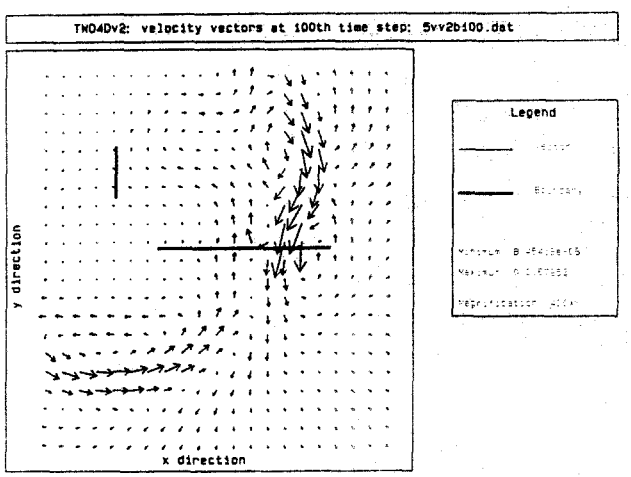

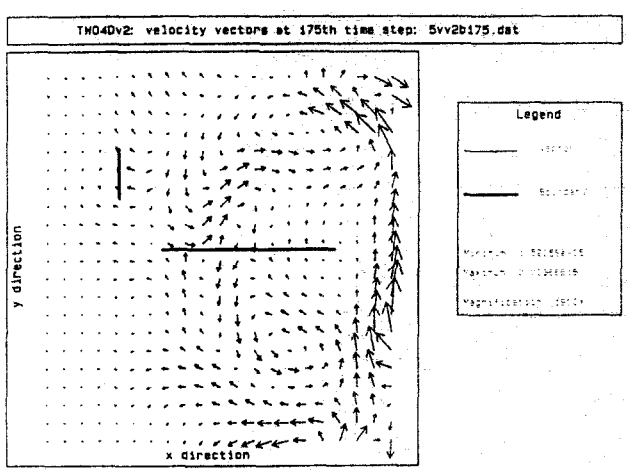

Figure 7. Snapshots in time of filled stope response.

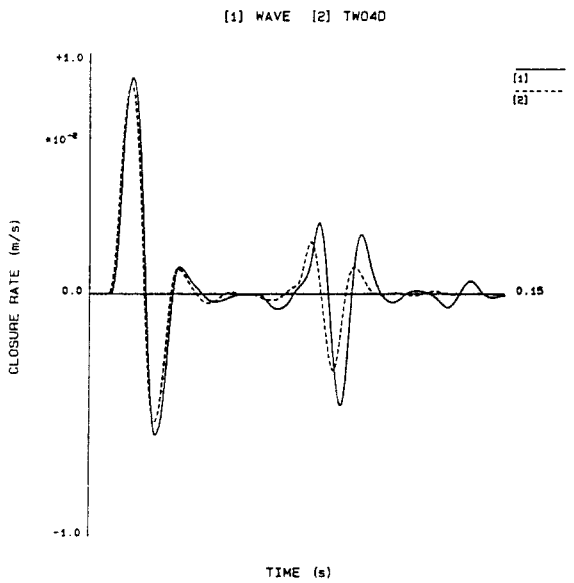

Figure 8. Normal velocity discontinuities at A for unfilled stope.

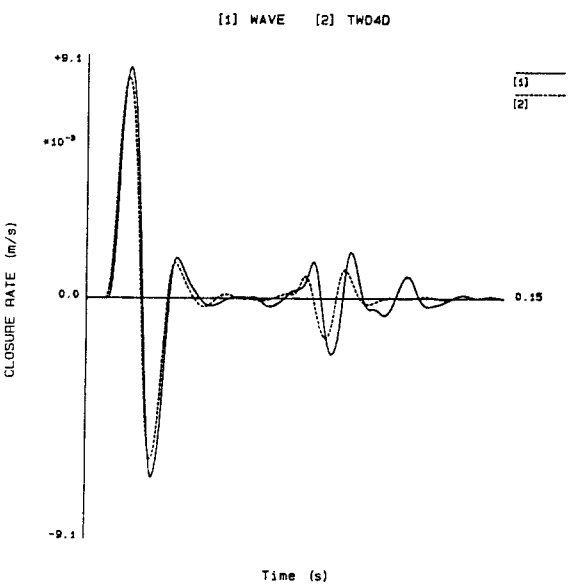

Figure 9. Normal velocity discontinuities at A for filled stope.

A diffracted wave, from the right hand-side stope face, is evident in Figure 7b. Figure 8 shows the closure rate (i.e. rate of change in normal component of displacement discontinuity) across the stope at position A (Figure 6) for the unfilled stope, and Figure 9 shows the effect of a filled stope. Figures 8 and 9 also contain the numerical results of an elastodynamic finite difference code, called WAVE [13], and the results are comparable with TWO4D. The wave reflection (arriving at $t \approx 0.7$ s) from the right-hand stope face is damped when backfill is introduced. A slight wave reflection (arriving at $t \approx 0.4$ s) is also evident from the edge of the backfill in the stope in the TWO4D results. A more detailed numerical study on the stability of backfilled stopes under dynamic excitation is available [14].

TWO REEF INTERACTION WITH DAYLIGHTING FAULT

A shear fault that daylights into two inclined stopes is shown in Figure 10. The entire fault is activated at time t = 0 by a simple Heaviside (in time) shear traction loading. This applied shear traction loading corresponds to the "static excess shear stress" developed along the line of the fault due to an initial compressive primitive stress field of 54 MPa vertically and 27 MPa horizontally, and assuming a Mohr-Coulomb failure criterion with cohesion 10 MPa and friction angle 30°. Static excess shear stress is the shear stress available to trigger a shear-based event [15]. The static excess shear stress is calculated, using an elastostatic displacement discontinuity method, for the case when only the two stopes exist in the rock mass. TWO4D is then used to determine the induced dynamic interactions between the two stopes and the fault, the driving force being the applied static excess shear stress obtained from the static calculation.

The dynamic friction angle and dynamic cohesion are assumed to be zero along the fault, which is a worst case scenario. In reality, a fault surface would have some residual friction during the dynamic phase. Special elements can be included to model frictional behavior. The normal traction along the fault is assumed to remain unchanged during the dynamic phase. The fault is assumed to have a normal stiffness of K_n = 50 GPa/m. The surrounding rock mass is assumed to have elastic constants of E = 70 GPa, ν = 0.2, and ρ = 2,700 kg/m^3.

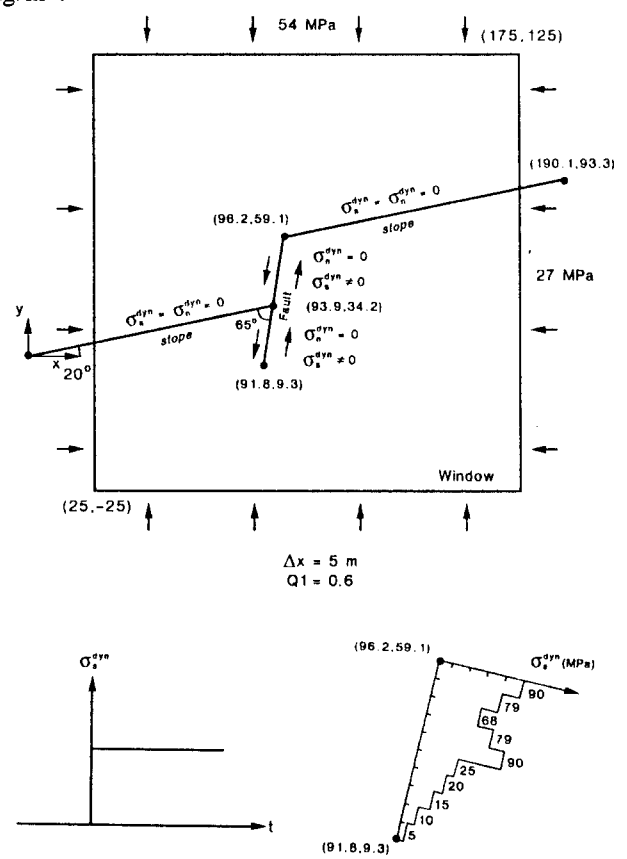

Figure 10. Stope-fault geometry and loading.

Figure 11 shows a snapshot in time of the dynamic displacement vectors on a vertical window. The two circular lobes are the shear waves moving out into the rock mass, away from the fault. The sense of shear along the fault is indicated by the displacement vectors at field points close to the fault. Figures 12 and 13 are snapshots in time of the induced dynamic principal stresses and the total (i.e. initial static plus dynamic) principal stresses, respectively. Figure 13 shows that the dynamic action is strong enough so that it is not swamped by the primitive stress field. This is evident from the local tensile zones (which change with time) and skewed orientations of the principal stress field (which also change with time) remote from the stopes and fault.

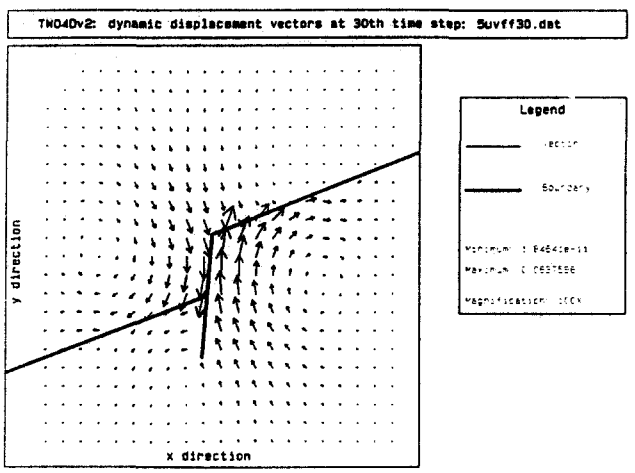

Figure 11. Dynamic displacement vectors at 30th time step.

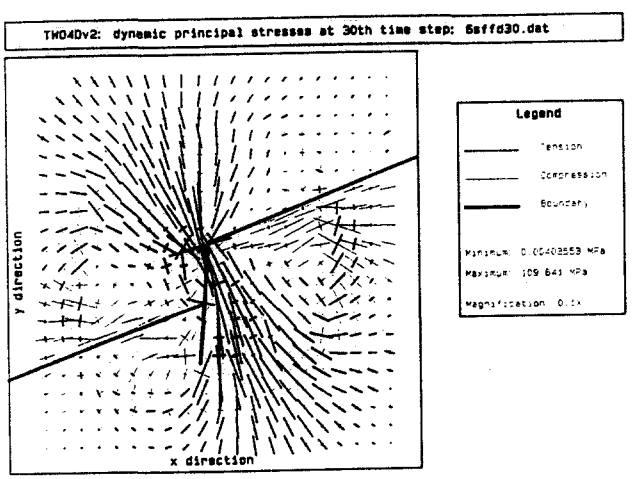

Figure 12. Induced dynamic principal stresses at 30th time step.

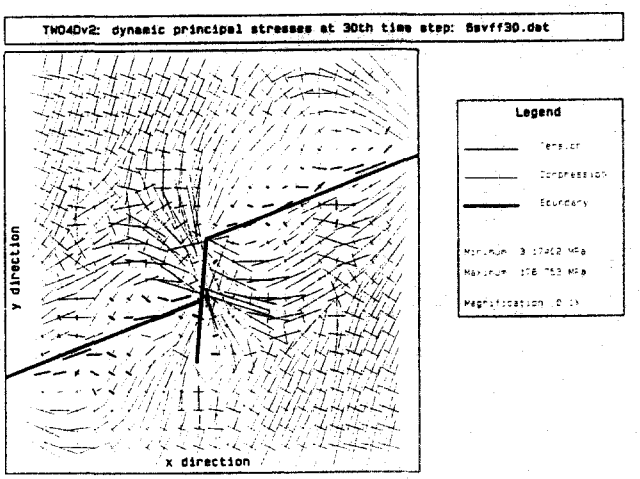

Figure 13. Total principal stresses at 30th time step.

ANTIPLANE STRAIN SLIP NEAR SURFACE OF HALF-PLANE

A displacement discontinuity element under antiplane strain conditions, has a non-zero out-of-plane displacement discontinuity component, and zero in-plane components. In other words, $D_z \neq 0$, and $D_x = D_y = 0$, where z is the axis of plane strain. A half plane problem can be modeled in an approximate way with the displacement discontinuity method, by introducing a line of elements representing the surface of the half plane. This representation provides a good approximation to the effects of the surface until the first diffractions from the edges of the truncated surface elements reach the field point(s) of interest.

Figure 14 shows a slipping Mode III crack that intersects with the surface of a half-plane. The inclined crack is loaded by applying a prescribed antiplane shear traction, as shown in Figure 14.

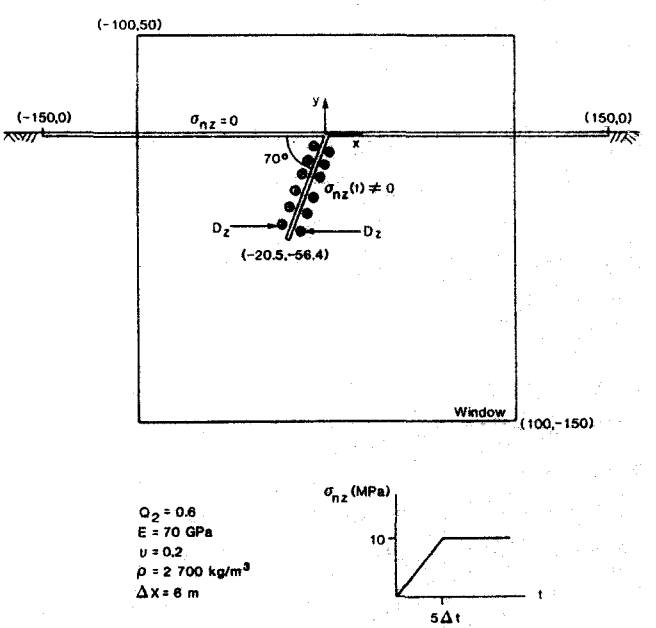

Figure 14. Antiplane strain problem geometry and loading.

The small circles containing either crosses or dots depicted in Figure 14 indicate the sense of antiplane shear.

Contours of the out-of-plane particle velocities v_z at the 40th time step are shown in Figure 15. The surface of the half plane has a significant effect on the location of the peak particle velocities. In the absence of the half plane, the particle velocities would be symmetric about the slipping crack, and attenuate away from the source. The introduction of the half plane allows surface waves and reflections to develop, thereby influencing the pattern of particle velocities.

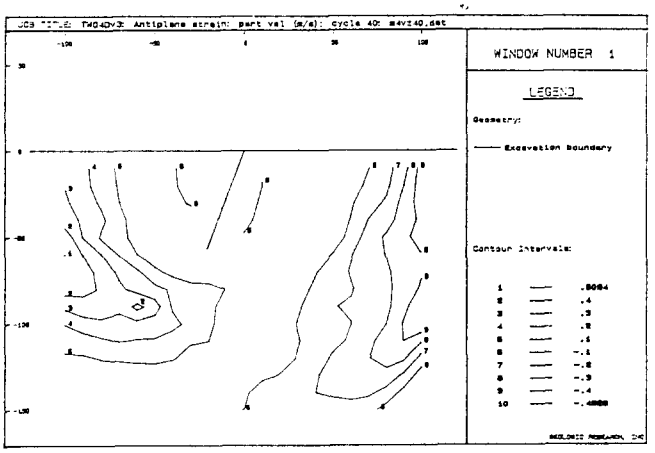

Figure 15. Particle velocity v_z contours at 40th time step.

CONCLUSIONS

A two-dimensional elastodynamic displacement discontinuity method has been used to model a variety of application problems. Both crack and cavity type geometries have been modeled, demonstrating the versatility of this method. The method can be extended to include any desired linear or non-linear material behavior within each element [7], provided that suitable dynamic constitutive relations can be found. The displacement discontinuity method can be combined with other boundary integral methods, such as [9], so that cavity type applications can be modeled more appropriately.

Future work on TWO4D will include the introduction of various friction laws for investigating active and passive fault movement, further stope support constructs, and an algorithm to allow normal and shear cracks to grow automatically, depending on the stress conditions ahead of the crack tip at each time step.

Acknowledgements—This work forms part of the research program into rock mass behavior of Mining Technology, a division of CSIR. The authors gratefully acknowledge CSIR for permission to publish this work. John Crouch of GeoLogic Research, Inc. and Mark Hildyard of CSIR provided all the graphics capabilities.

REFERENCES

1. Crouch, S.L. and Starfield, A.M. *Boundary Element Methods in Solid Mechanics,* George Allen and Unwin, London (1983).
2. Das, S. and Aki, K. A numerical study of two-dimensional spontaneous rupture propagation, *Geophys. J. astro. Soc.,* 50, 643-668 (1977).
3. Andrews, D.J. Dynamic plane-strain shear rupture with a slip-weakening friction law calculated by a boundary integral method, *Bull. Seism. Soc. Am.,* 75, 1-21 (1985).
4. Das, S. and Kostrov, B.V. On the numerical boundary integral equation method for three-dimensional dynamic shear crack problems, *J . of Appl. Mech.,* 54, 99-104 (1987).
5. Hirose, S. and Achenbach, J.D. Time-domain boundary element analysis of elastic wave interaction with a crack, *Int. J. Num. Meth. Engng.,* 28, 629-644 (1989).
6. Mack, M.G. A three-dimensional boundary element method for elastodynamics, *Ph.D. dissertation,* University of Minnesota (1991).
7. Siebrits, E. Two-dimensional time domain elastodynamic displacement discontinuity method with mining applications, *Ph.D. dissertation*, University of Minnesota (1992).
8. Eringen, A.C. and Suhubi, E.S. *Elastodynamics II: Linear theory*, Academic Press, New York (1975).
9. Tian, Y. Boundary element methods in elastodynamics, *Ph.D. dissertation*, University of Minnesota (1990).
10. Freund, L.B. *Dynamic Fracture Mechanics*, Cambridge Press, New York (1990).
11. Loken, M.C. A three-dimensional boundary element method for linear elastodynamics, *Ph.D. dissertation*, University of Minnesota (1992).
12. Gurtunca, R.G. and Adams, D.J. Determination of the in situ modulus of the rock mass by the use of backfill measurements, *J. S. Afr. Inst. Min. Metall.*, 91, 81-88 (1991).
13. Cundall, P.A. Program WAVE, personal communication (1990).
14. Siebrits, E., Hildyard, M.W. and Hemp, D.A. Stability of backfilled stopes under dynamic excitation, subm: *Proc. 3rd Int. Symp. on Rockbursts and Seismicity in Mines, Kingston,* Balkema, Rotterdam (1993).
15. Ryder, J.A.R. Excess Shear Stress (ESS): An engineering criterion for assessing unstable slip and associated rockburst hazards. eds: G. Herget and S. Vongpaisal, proc: *6th Int. Congress on Rock Mechanics,* ISRM, Balkema, Rotterdam (1987).